Journal of Environmental Management 374 (2025) 124021

Contents lists available at ScienceDirect

Journal of Environmental Management

journal homepage: www.elsevier.com/locate/jenvman

Research article

High-resolution assessment of climate change impacts on the surface energy and water balance in the glaciated Naryn River basin, Central Asia

Sanjar Sadyrov [a,c,*], Erkin Isaev [b], Kenji Tanaka [c], Akihiko Murata [d], Roy C. Sidle [a]

[a] Mountain Societies Research Institute, University of Central Asia, Bishkek, Kyrgyzstan
[b] Scientific and Technical Council, Hydrometeorological Service of Kyrgyzstan, Bishkek, Kyrgyzstan
[c] Disaster Prevention Research Institute, Kyoto University, Uji, Kyoto, Japan
[d] Meteorological Research Institute, Tsukuba, Japan

ARTICLE INFO

Keywords:
Snowmelt
Glaciers
Hydrological modeling
Naryn river
Central Asia

ABSTRACT

Mountain regions of Central Asia are experiencing strong influences from climate change, with significant reductions in snow cover and glacial reserves. A comprehensive assessment of the potential consequences under the worst-case climate scenario is vital for adaptation measures throughout the region. Water balance analysis in the Naryn River basin was conducted for the baseline period of 1981–2000 including potential changes under the worst-case SSP5-8.5 scenario for 2077–2096 by combining high-resolution (5 km) regional climate projections with fully distributed glacio-hydrological (1 km) modeling. Results showed that with the complete degradation of glaciers and increase in evapotranspiration, the overall runoff will decrease by 16%, and in the upper basins, the reduction will exceed 40%. The maximum snow water equivalent (SWE) is projected to decrease by 17%, and the seasonal peak of SWE will occur one month earlier. The transition from snow to rain will significantly affect lower regions, increasing extremes in peak runoff and causing 10-year recurrence interval events to occur every 3–4 years. Moreover, extreme runoff in high mountainous areas will increase due to intensified snowmelt and increased rainfall extremes. Additionally, a gradient of surface soil temperature change of 0.1 °C per 100 m elevation gain was observed, suggesting a potential snow-albedo feedback effect that could further amplify the warming, especially at higher altitudes. This study provides a robust analytical framework to assess the complex responses of mountain ecosystems to the impacts of climate change, with the potential of widespread application for addressing the challenges facing these critical regions.

1. Introduction

The Central Asian region, particularly the Tien Shan, is highly dependent on glaciers and snowmelt as principal water resources for the local semi-arid environment, and this dependence is being profoundly impacted by climate change, marked by rising temperatures, shrinking glaciers, altered precipitation patterns, and increased risk of natural hazards (Siegfried et al., 2012; Schaner et al., 2012; Chen et al., 2016; Barandun et al., 2020). Climate change is affecting cryosphere water sources, with glaciers in the region experiencing substantial mass loss in recent decades (Farinotti et al., 2015; Huss and Hock, 2018). The Naryn River basin, located in the central Tien Shan of Kyrgyzstan, is a crucial contributor to the Syr Darya River, which supplies water for agriculture and transboundary users downstream Uzbekistan in the Fergana Valley and then to Kazakhstan where it eventually discharges into the Aral Sea (Wegerich et al., 2015; Hill et al., 2017; Zou et al., 2019). Studies have reported increasing trends in Naryn River discharge, which have been attributed to enhanced glacier and snowmelt due to rising temperatures (Podrezov, 2001; Kriegel et al., 2013; Gan et al., 2015; Zou et al., 2019; Saks et al., 2022; Shannon et al., 2023; Kalashnikova et al., 2023). The relative contribution of glacier meltwater to the overall discharge of the Naryn River remains a topic of uncertainty and active investigation (Unger-Shayesteh et al., 2013). Understanding the dynamics of glacier melt and its impact on river runoff is crucial for managing water resources and adapting to climate change in this water-stressed region (Chen et al., 2017; Pohl et al., 2017).

Central Asia has been experiencing a trend towards increased temperature and precipitation, with the region getting warmer and wetter during the past 80 years (Yan et al., 2022) and will continue under various Global Climate Models (GCMs) provided by Coupled Model

* Corresponding author. Mountain Societies Research Institute, University of Central Asia, Bishkek, Kyrgyzstan.
E-mail address: sanjar.sadyrov@ucentralasia.org (S. Sadyrov).

https://doi.org/10.1016/j.jenvman.2024.124021
Received 14 October 2024; Received in revised form 3 December 2024; Accepted 31 December 2024
Available online 9 January 2025
0301-4797/

Intercomparison Project Phase 6 (CMIP6) (Cao et al., 2023). Mountainous regions of Central Asia, particularly in Kyrgyzstan and Tajikistan, are identified as highly vulnerable to climate change, where a projected warming trend of 6 °C is expected under the Shared Socioeconomic Pathway (SSP) scenario SSP5-8.5 from 2076 to 2096 (Isaev et al., 2024). The projected retreat of glaciers in the Tien Shan, as indicated by modeling results, further exacerbates climate change impacts with the timing and magnitude of melt varying depending on specific climatic conditions, precipitation patterns, and geographic characteristics of each individual ice body (Rupper et al., 2009; Van Tricht and Huybrechts, 2023). By 2100, only 8% of the areal extent of small glaciers in Naryn River basin inventoried during the baseline period (1966–1995) will remain under the Representative Concentration Pathway 8.5 (RCP8.5) scenario with a projected decrease in total runoff by 1%, 6% and 17% by the end of the century for RCP2.6, RCP4.5, RCP8.5, respectively (Gan et al., 2015). The projections of six ice masses in the Tien Shan up to 2100 reveal that, under all climate scenarios, the ice masses become significantly smaller, with most of the ice masses disappearing altogether under the SSP5-8.5 scenario (Van Tricht and Huybrechts, 2023).

The Naryn River basin experiences a substantial contribution of glacier melting to the overall runoff. In the highly glacierized Naryn headwater sub-catchment, it has been observed that glacier melting accounts for as much as 66% of the total runoff in August (Shannon et al., 2023). Snowmelt is by far the dominant annual water supply to the Naryn and Karadarya rivers, with approximately 70% of water for irrigated agriculture in the Fergana Valley originating from snow-ice sources (Radchenko et al., 2014). Earliest estimates by Aizen et al. (1995) indicate that for the broader Naryn catchment, glacier melt roughly supplied 10% of the total annual discharge during the period of 1940–1991; later research suggested a 6% contribution from 1956 to 2007 (Gan et al., 2015), indicating lower glacial melt contributions to total runoff. However, glacial contributions in upper sub-catchments contribute an average of 23% of total annual runoff (Saks et al., 2022).

Most runoff studies use conceptual hydrologic models to assess the impact of climate change on water resources, as these require less input data and computing time compared to physically-based models (Seiller et al., 2012; Bai et al., 2015, 2018; Fowler et al., 2016; Saft et al., 2016). However, the calibrated model parameters generally lose their physical representation due to equifinality (Beven and Freer, 2001; Beven, 2006), which is particularly challenging in the context of climate change assessments and overall modeling strategies (Her et al., 2019; Sidle, 2021). There is increasing evidence that the robustness of hydrologic models decreases when they are applied to climatic conditions that differ from the periods used for calibration (Coron et al., 2012; Thirel et al., 2015; Fowler et al., 2016). This raises a concern that models calibrated using historical data may become unreliable in projecting future runoff regimes due to the differences in climate between the historical period and the future. However, this potential uncertainty is often overlooked when assessing the impacts of climate change on water resources, leading to an underestimation of the uncertainty in future runoff projections (Wilby and Harris, 2006; Barron et al., 2012; Verzano et al., 2012). Additionally, the coarser temporal resolution and the fixed degree day parameters used in simpler melt models make them more controversial for application in climate change studies compared to more complex energy-balance models (Carletti et al., 2022). The simplified assumptions and lower computational demands of conceptual models come at the cost of potentially reduced accuracy and physical relevance when projecting the impacts of climate change on water resources.

In High Mountain Central Asia, it is particularly important to consider ice melting processes in hydrological modeling, as glacier melt is one of the most significant water sources for glaciated basins in the region (Chen et al., 2017; Sadyrov et al., 2024). Considering that climatic forcing has been identified as the dominant driver for the heterogeneous mass balance sensitivity across Central Asia (Barandun and Pohl, 2023) and High Mountain Asia, accounting for up to 60% of the spatially contrasting glacier response in the region (Sakai and Fujita, 2017), it is crucial to represent local climate at a finer spatial resolution. Dynamical downscaling, which involves nesting a high-resolution Regional Climate Model (RCM) within a coarser-resolution GCM, has been proposed as a valuable approach to enhance the accuracy of hydrological simulations and improve the understanding of climate change impacts on river basins (Hasson et al., 2014).

In this study, we employ a comprehensive approach by utilizing advanced high-resolution fully distributed (1 km) land surface and glaciological energy and mass balance modeling. The models will be driven by dynamic downscaled climate forcing data obtained from a non-hydrostatic regional climate model (NHRCM) (5 km) previously assessed in Central Asia (Isaev et al., 2024), allowing us to estimate changes in runoff patterns within Naryn River Basin focusing on the impacts of glacier retreat, seasonal snowmelt shifts, increased evapotranspiration, and other relevant variables. We compare modeling outputs from the baseline period (1981–2000) with future projections (2077–2096) under the worst-case SSP5-8.5 climate change scenarios, considering complete degradation of glaciers by the end of this century. To evaluate variations in total runoff and understand the potential buffering effect of glaciated areas, we use a total runoff standardized anomaly index (TR-SAI) in our analysis, allowing us to assess the deviations in runoff patterns and identify any changes that may occur in the future.

2. Methods

2.1. Study area

The study area encompasses the upper Naryn River basin upstream of Uchterek, inflow point to the Toktugul Reservoir in Kyrgyzstan, and its sub-basins, namely Chon-Naryn (Big Naryn) and Kichi-Naryn (Small Naryn). Chon-Naryn covers 5546 km^2, Kichi covers 3870 km^2, and the main Naryn River (upstream of Uchterek) basin covers 46,188 km^2. Glaciers cover 8.6% (477.7 km^2) and 7.4% (287 km^2) of the Chon-Naryn and Kichi sub-basins, respectively. Glacial cover in the Naryn River basin is 2.3% (1047 km^2).

Naryn River basin experiences a severe continental climate where winter temperatures can plummet below −50 °C while summer temperatures can exceed 40 °C (Hill et al., 2017). Average temperatures typically range from −15 °C to 20 °C (Fig. S1). The diverse climate within the basin is primarily influenced by elevation, complex mountainous terrain, mountain exposure, incised valleys, and the presence of mountain glaciers and lakes. These factors contribute to differences in solar radiation and atmospheric moisture, ultimately leading to vertical differentiation of the climate within the basin. Within Kyrgyzstan, the basin is characterized by climate zones ranging from the foothill plains and low-lying valleys (900 m–1500 m) to the sub-alpine (1500 m–2500 m), alpine (2500 m–3500 m), and finally the glacial-nival climate zone (>3500 m).

2.2. Meteorological forcing from regional climate model

We used the non-hydrostatic regional climate model (NHRCM) developed by the Meteorological Research Institute (MRI) of the Japan Meteorological Agency (JMA) (Sasaki et al., 2008) which was adapted for Central Asia (NHRCM-CA; Isaev et al., 2024). High-resolution (5 km) climate projections were validated and compared to CMIP6 General Circulation Models and Coordinated Regional Climate Downscaling Experiment (CORDEX) regional models. Additionally, to assess future temperature anomalies and the statistical significance of these changes, we utilized a bootstrap method where future temperature and precipitation anomalies were estimated by generating 10,000 bootstrap samples created by randomly selecting and replacing data from a 20-y dataset. To validate historical baseline projections, we used monthly precipitation and monthly mean air temperature data from meteorological stations in Tian-Shan, Naryn, Chaek, and Suusamyr (Fig. 1) covering the period from 1940 to 2020 (Fig. S2). In this study, the temperature data from regional climate model was downscaled using the specified temperature lapse rate of 6.0 °C km^{-1}, close to the observed rate of 5.8 °C km^{-1} in the Tien-Shan mountains (Aizen and Aizen, 1997).

2.3. Models

Hydrological assessment of runoff sources in high mountain areas is crucial for understanding water availability in these ecologically sensitive regions. High spatial and temporal resolution modeling techniques have the potential to provide valuable insights into the complex dynamics of runoff sources, including rainfall, snowmelt runoff, and glacier melt. With their ability to capture fine-scale variations in topography, land cover, and climate factors, high-resolution models offer improved understanding of the spatial distribution of runoff sources, as well as evapotranspiration processes.

2.3.1. Land surface model

The Simple Biosphere including the Urban Canopy (SiBUC) model is a land surface model that uses a water-energy balance approach within a grid system (Tanaka, 2004). It is based on the earlier Simple Biosphere (SiB) (Sellers et al., 1986) and SiB2 (Sellers et al., 1996) models. SiBUC integrates various processes for different mosaic schemes including green areas, water bodies, and urban areas. The mosaic scheme was enhanced by incorporating a separate routine to model glacier processes (Fig. 2), which has been shown to improve the system's overall understanding in mountainous environments (Zhao et al., 2013). To accommodate a coarser resolution in the model, the linear relationship between snow cover fraction (SCF) and snow water equivalent has been modified to allow for the rapid establishment of snow cover in small-scale simulations (Niu and Yang, 2007). The snowmelt process is strongly influenced by thermodynamics of the snowpack, and this relationship is described by the following governing equation:

$$C_s\frac{\partial T_s}{\partial t} = Rn_g - H_g - \lambda E_g - K_s\frac{T_s - T_g}{D_s} \tag{1}$$

where C_s is a heat capacity of the snow (J m^{-2} K^{-1}), T_s is a snow surface temperature (K), Rn_g is absorbed net radiation (W m^{-2}), H_g is sensible heat flux (W m^{-2}), λE_g is latent heat flux (W m^{-2}), K_s is snow thermal conductivity (W m^{-1} K^{-1}), T_g is ground surface temperature (K), and D_s is snow depth (m). The snow depth is calculated from snow water equivalent considering a constant snow density of 200 kg/m^3. The SiBUC model estimation of snow albedo (the reflectivity of snow) is

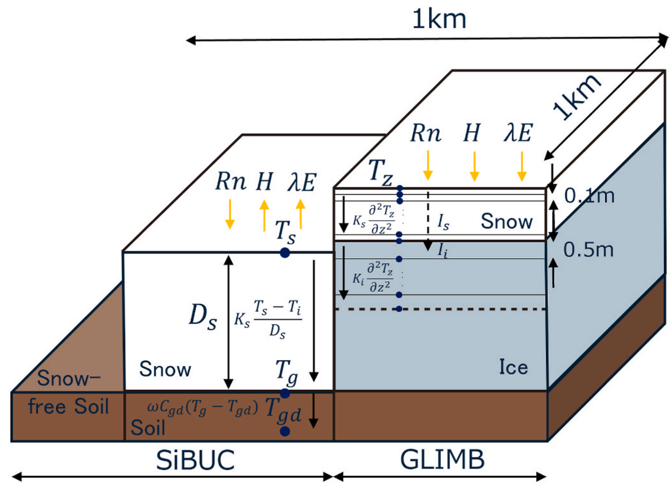

Fig. 2. Representation of land surface and glacier models in a mosaic 1 km scale.

based on an approach that accounts for the gradual aging and evolution of the snow cover (Kondo and Xu, 1997):

$$a_d = (a_{d-1} - a_f)e^{-\frac{1}{k}} + a_f \tag{2}$$

In the event of snowfall exceeding 5 mm snow water equivalent (SWE), the number of days (d) is reset to 0. The albedo of firn (0.45) is represented by a_f, while the albedo of fresh snow (0.81) is denoted as a_0. Additionally, the parameter k is influenced by daily air temperature.

Land surface parameters used in the model include land-cover fractions determined from the GLCC ver2.0 (Loveland et al., 2000) 1-km gridded dataset provided by USGS. Soil physical parameters are identified using a 1-km Ecoclimap from Meteo-France (Champeaux et al., 2005). The GTOPO30 (1 km) dataset was used as Digital Elevation Model (DEM) data. All model parameters can be determined using land-surface products, eliminating the need for calibration. Soil characteristic parameters in SiBUC are based on Cosby et al. (1984).

2.3.2. Glacier model

We used the glacier energy-mass balance model (GLIMB) to incorporate glacier processes, which has previously been applied to investigate glaciers of High Mountain Asia (Fujita and Ageta, 2000; Fujita and Sakai, 2014) and the inner Tien Shan region (Fujita et al., 2011; Sadyrov et al., 2024). By utilizing reanalysis data and in-situ observations, this

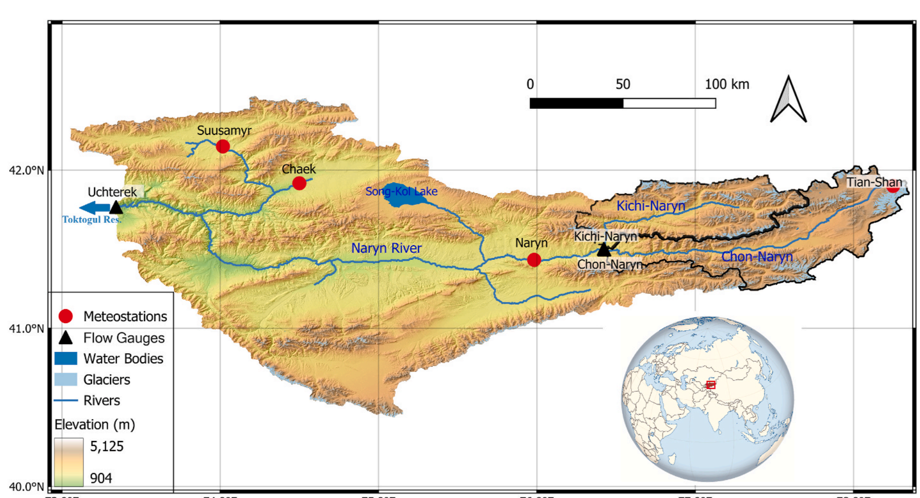

Fig. 1. Naryn River Basin and locations of meteorological stations and flow gauges.

model successfully demonstrated the effectiveness of an energy balance approach in modeling mass balance within complex mountainous environments. Glacier runoff (D_g) is calculated as:

$$D_g = \frac{t_{day}Q_s}{l_m} + P_r + \left[\frac{H_L}{l_e}, 0\right] - R_f \tag{3}$$

where R_f is a refrozen water in a snow layer when it percolates into cold snow, t_{day} is a length of a day in seconds, l_m is a latent heat fusion of ice, P_r is a rainfall (mm), l_e is a latent heat of evaporation of water. The distinction of snow (P_s) and rain from total precipitation (P_p) is based on air temperature (T_a) and assumed as follows:

$$P_s = P_p \quad [T_a \leq 0.0^\circ C], \tag{4}$$

$$P_s = \left(1 - \frac{T_a}{4.0}\right)P_p \quad [0.0^\circ C < T_a < 4.0^\circ C], \tag{5}$$

$$P_s = 0 \quad [T_a \geq 4.0^\circ C], \tag{6}$$

$$P_r = P_p - P_s. \tag{7}$$

While surface heat (Q_s) is derived by the following:

$$Q_s = (1 - a_s)H_{SR} + H_{LR} - \varepsilon\sigma(T_s + 273.15)^4 + H_S + H_L - G_g \tag{8}$$

Ice surface albedo (a_s) is an assumed constant mean value of 0.25 determined by automatic weather stations located in the area and instrumental albedo measurements (Petrakov et al., 2019; Sadyrov et al., 2024). While the measurements were conducted between 2017 and 2023, we extrapolate these values as representative of all glaciers within the region. H_{SR}, H_{LR}, H_S, *and* H_L refer to the downward shortwave, longwave radiations, sensible and latent heat fluxes, respectively. Additionally, G_g represents the conductive heat flux into the glacier ice, which is determined based on the variations in the ice temperature profile. The turbulent sensible heat flux (H_S) and latent heat flux (H_L) were estimated using the bulk aerodynamic method. In this approach, the gradients of mean horizontal wind speed (U), mean air temperature (T), and mean specific humidity (q) were assumed to be equivalent to the finite difference between the measurement level and the surface:

$$H_s = \rho C_p U C_s (T - T_s) \tag{9}$$

$$H_L = \rho l_f U C_L (q - q_s) \tag{10}$$

In the equation, ρ represents air density, C_p denotes specific heat capacity of air, T_s is surface temperature, and q_s is specific humidity at the surface. Additionally, U represents wind speed, l_f corresponds to the latent heat of evaporation (2.514×10^6 J kg^{-1}) or sublimation (2.849×10^6 J kg^{-1}), depending on the surface temperature. The bulk exchange coefficients for sensible heat (C_s) and latent heat (C_L) were assumed to be constant at 0.002. This decision was made due to the limited availability of information regarding surface roughness and wind profiles over snow and ice. The heat balance equations for the snow layer, and ice layer are described by:

$$\rho_s c_s \frac{\partial T_z}{\partial t} = K_s \frac{\partial^2 T_z}{\partial z^2} + \frac{\partial I_s}{\partial z} \tag{11}$$

$$\rho_i c_i \frac{\partial T_z}{\partial t} = K_i \frac{\partial^2 T_z}{\partial z^2} + \frac{\partial I_i}{\partial z} \tag{12}$$

where ρ_x represents snow (s) and ice (i) densities (kg m^{-3}), c_x is the heat capacity of snow and ice (J K^{-1} kg^{-1}), T_z is temperature at depth (z)(°C), and I_x is transmitted solar radiation (W m^{-2}). Thermal conductivities K_s (snow) and K_i (ice) (W m^{-1} K^{-1}) are determined by:

$$K_s = 0.029\left(1 + 10^{-4}{\rho_s}^2\right) \tag{13}$$

$$K_i = \frac{488.2}{T_z} + 0.47 \tag{14}$$

The snow and ice layers are multi-layered, with a snow layer thickness of 0.1 m and an underlying ice layer thickness of 0.5 m. The process of consolidation is considered in the model. Additionally, refreezing of seepage water and the formation of ice accumulation are considered. Mosaic fractionation of the glacier was determined by integrating the vector shape of the glacier outlines sourced from the GAMDAM Glacier Inventory (Nuimura et al., 2015; Sakai, 2019) integrated into the global glacier inventory (Randolph Glacier Inventory (RGI) version 6.0, RGI--Consortium, 2017). As a result, the glaciated fraction within each 1-km grid varies from 0.01 to 1 and total runoff from the grid is respectively calculated. In the context of projecting future climate scenarios, the analysis excluded the glacier component to simulate the complete disappearance of glacier coverage. This approach was motivated by the unavailability of consistently high-resolution forcing data needed to model a gradual decline in glacier extent and volume, thereby minimizing uncertainties associated with varying ice thickness estimations.

2.4. Total runoff standardized anomaly index (TR-SAI)

The ability to accurately predict irregular or unexpected changes in total runoff is crucial, particularly in the context of climate change. Glaciers have a buffering effect that helps regulate streamflow during dry years, by supplying water during dry seasons, acting as a stabilizing influence (Pritchard, 2017; Pohl et al., 2017). However, the observed trend of glacier degradation poses a threat to this buffering capacity, which can affect crop productivity in the region (Park et al., 2021; Chang et al., 2024). The Total Runoff Standardized Anomaly Index (TR-SAI) was proposed, drawing inspiration from the Standardized Precipitation Index (SPI) methodology (McKee et al., 1993), providing a standardized measure of the deviation of hydrologic runoff from the norm.

$$TR - SAI_i = \frac{Total\ runoff_i - Total\ runoff_{mean}}{\sigma} \tag{15}$$

This index was applied in a gridded scale for each historical baseline year (i) and compared to projected years (j) considering future conditions as:

$$TR - SAI_j = \frac{Total\ runoff_j - Total\ runoff_{mean}}{\sigma} \tag{16}$$

The mean total runoff and standard deviation (σ) were obtained from baseline historical values. Positive TR-SAI values indicate above-normal runoff conditions, while negative values indicate below-normal conditions.

3. Results

3.1. Analysis of precipitation and temperature changes

The NHRCM-CA model predicts that in most of the Naryn River basin, the annual mean temperature will increase by more than 6 °C (Fig. 3a). For the SSP5-8.5 scenario, both annual mean temperature (Fig. 3a) and seasonal mean temperature (Fig. 4) are projected to rise throughout the entire Naryn River basin. For all meteorological stations, there is a projected increase of >5 °C in monthly temperature, and all changes are statistically significant (Fig. 5a). Furthermore, significant increases in projected monthly precipitation anomalies are mainly observed during the spring and winter months (Fig. 5b).

3.2. Total runoff difference

Simulations of the spatial distribution of surface runoff in Naryn River basin in a changing climate (SSP5-8.5 scenario) reveal significant

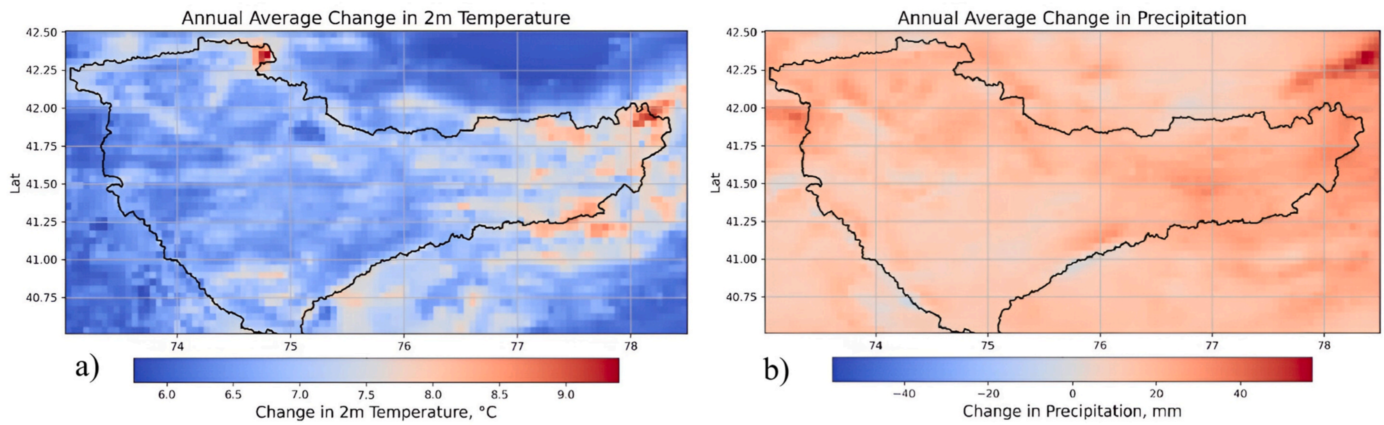

Fig. 3. Future changes of a) annual mean temperature anomalies (°C) and b) changes in total annual precipitation (mm) during 2076–2096 across Naryn River basin derived from NHRCM-CA under the SSP5-8.5 scenario, base period: 1980–2000.

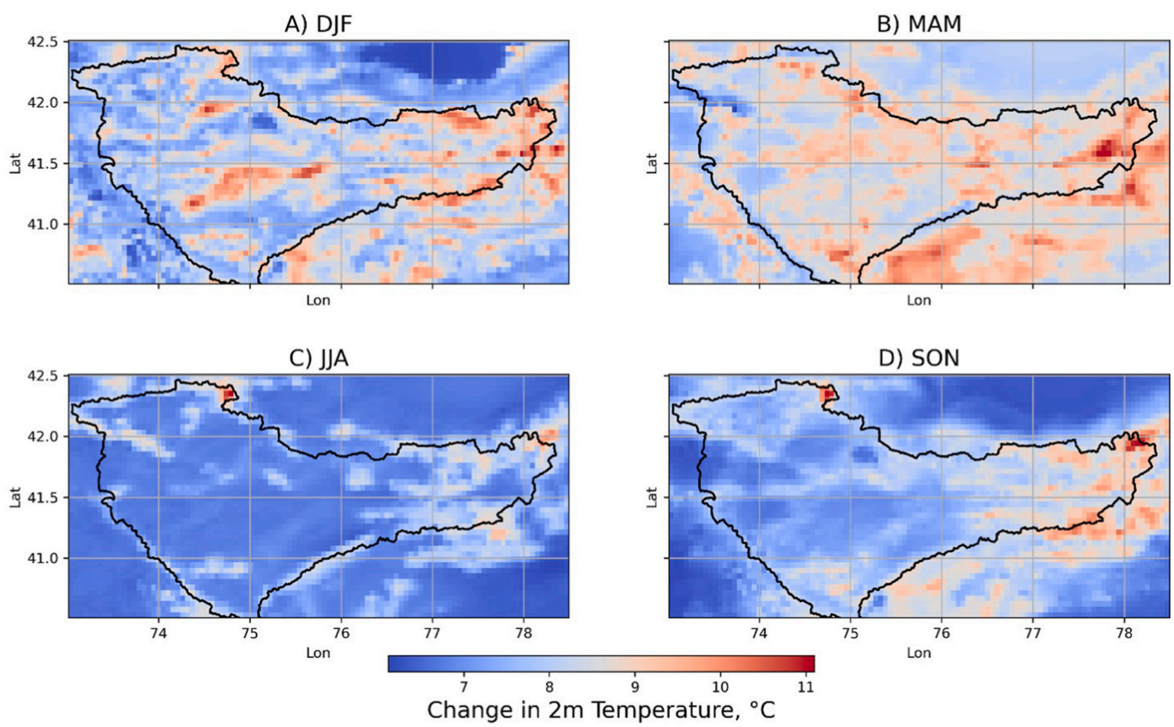

Fig. 4. Future changes of seasonal mean temperature anomalies (°C) during 2076–2096 across Naryn River basin derived from NHRCM-CA under the SSP5-8.5 scenario compared to base period seasons: 1980–2000; a) DJF (Dec., Jan., Feb.); b) MAM (Mar., Apr., May); c) JJA (Jun., Jul., Aug.); and d) SON (Sep/. Oct., Nov.).

variations in different regions (Fig. 6). Notably, the western region near the Fergana Range and Toktogul Reservoir emerges as a more humid area by the end of the 21st Century with certain locations experiencing substantial increases in total runoff (exceeding 100 mm; Fig. 6a). These effects predominantly occur in the lower basin. In future simulations where glacial cover was deliberately excluded under the worst-case climate scenario, we could observe the direct effects on total runoff in the glacier grids. This simulation showed a remarkable reduction of >150 mm of runoff, ultimately reaching ≈1000 mm. These findings have profound implications for the availability of water runoff in high mountain glaciated areas.

The analysis of surface soil temperature reveals variations in temperature changes across elevation (Fig. 6c) and the region with an average increase of 8 °C (Fig. 6b). Lower-lying areas exhibit relatively smaller differences in these values compared to high mountain regions. The primary factors contributing to such disparities are the significant reduction in snow cover duration and depth, especially at higher altitudes, resulting in an increased radiation balance. At an elevation of 1400 m, the temperature difference was 6.9 °C, while at 2000 m the difference was 7.6 °C. At 3000, 4000, and 4800 m, the temperature differences were 8.4, 9.0, and 10.4 °C, respectively. Therefore, temperature gradient differences in surface soil averaged 0.1 °C per 100 m, which may also be associated with varying air temperature changes at different elevations, emphasizing potential impact of the snow albedo and melt feedback loop with a concomitant mean basin decrease in albedo by 18%.

3.3. Runoff difference by components

The analysis of runoff sources in the Naryn Uchterek (inflow to Toktogul reservoir) basin from 1981 to 2000 reveals notable variations in their contributions (Fig. 7). On average, rainfall constitutes

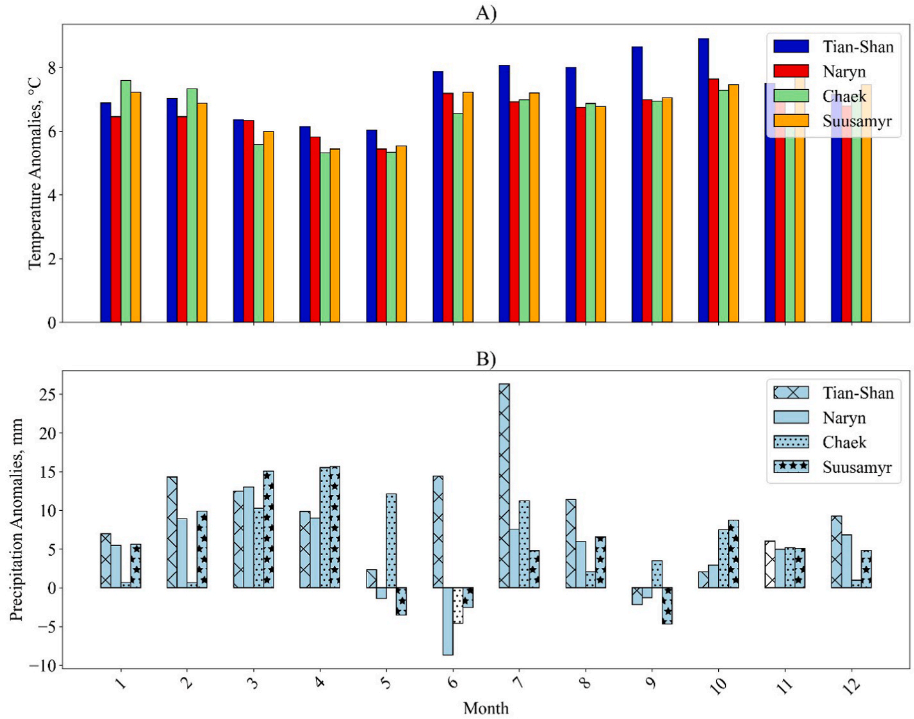

Fig. 5. Future changes of a) monthly mean temperature anomalies (°C) and b) monthly precipitation anomalies (mm) during 2076–2096 derived from NHRCM-CA under the SSP5-8.5 scenario, base period: 1980–2000; all temperature anomalies are statistically significant, light blue bars in (b) indicate statistically significant precipitation anomalies p-level <0.05 (estimated using 10,000 bootstrap samples with random replacement of the 20-y dataset).

approximately 25% of total runoff, while snowmelt runoff dominates with a mean contribution of 68%. Glaciermelt runoff, although relatively smaller, accounts for approximately 7% of the total runoff, reaching up to 14% in some years. In the Chon-Naryn basin, the distribution of runoff sources exhibits distinct characteristics. Rainfall contributes 14% of mean total runoff, while snowmelt runoff constitutes a significant mean contribution of 64%. Notably, glaciermelt runoff plays a more substantial role in this basin, accounting for approximately 22% of the total runoff and reaching up to 38% in some years. Similarly, in the Kichi-Naryn basin, rainfall contributes, on average, 12% of total runoff. Snowmelt runoff, similar to the other basins, plays a dominant role, accounting for 64% of the mean total runoff. Glaciermelt runoff, although relatively smaller in comparison, constitutes approximately 24% of the total runoff, reaching up to 37% in certain instances. The dominance of snowmelt runoff highlights the vulnerability of these basins to changes in snow accumulation, snow water equivalent, and melt patterns.

The analysis of evaporation (including also transpiration for non-glaciated grids) across different elevation zones reveals regional differences in variability (Fig. 8a) attributable to factors such as the availability of moisture for direct evaporation, which is explicitly considered in the model. Average evaporation values are similar at different elevations (1200–2400 m), ranging from 240 to 250 mm, dependent on the spatial distribution of precipitation and characteristics of the basin. However, a significant gradient of decreasing evaporation is evident above 2800 m, where the values reach 275 mm, and further decrease to 23 mm at an elevation of 4600 m. Beyond this threshold, we observe zero values of evaporation.

By utilizing meteorological data from the high-resolution climate projection under the SSP5-8.5 scenario, we analyzed modeled changes in evaporation across all elevation zones within the Naryn River basin. On average, evaporation has increased by 33% throughout the entire basin. For instance, in the 4200 m elevation zone, evaporation increased from 103 mm (base period) to 213 mm (future projections), representing a 107% increase under the most extreme climate change scenario. This trend is attributed to the diminishing snowpack and the degradation of glaciers. Our model accounts for the presence or absence of ice cover and surface albedo, which influence the radiative balance, leading to enhanced evaporation.

The analysis of rainfall runoff indicates elevational differences within the entire basin (Fig. 8b). Up to 2500 m, runoff predictions are relatively uniform, but variability increases with altitude due to the transition between rain and snow that is influenced by temperature fluctuations. Above 2500 m there is a gradual decrease in the amount of liquid precipitation and an increase in the snow. Minimum rainfall runoff occurs at elevations above 4200 m, attributed to sub-zero temperatures during much of the year. Consequently, the variability of rainfall runoff ranges from 180 mm at 2600 m to 17 mm at 4200 m, with an average gradient of −10 mm/100 m.

When comparing future changes of rainfall runoff with the baseline period in the context of the SSP5-8.5 climate scenario, the zonal distribution of rainfall runoff within the Naryn River basin remains relatively stable (Fig. 8b). However, there is a noticeable increase in variability at mid-high elevations (2600–4000 m), primarily attributed to the surge in rainfall runoff. This phenomenon manifests in a substantial 71% increase in rainfall runoff at the 2600 m elevation and a remarkable 102% increase across the entire basin. Notably, at 3800 m, rainfall runoff increases from 41 mm to 171 mm. The rate of rainfall runoff decrease with increasing elevation is relatively consistent at −9.9 mm/100 m, albeit with heightened variability. Notably, a change in the rainfall runoff-altitude relationship occurred in the upper zone, with a shift of about 1000 m in altitude, implying that in the most adverse climate change scenario, the amount of rainfall that is projected to be received at 3600 m is now comparable to what previously fell at 2600 m.

The contribution of snowmelt to the overall runoff in the Naryn River basin presents an interesting trend (Fig. 8c). The high-resolution modeling and precipitation input (Table 1) provide valuable insights into the relatively equal proportion of snowmelt runoff between elevation zones up to 2200 m. Thereafter, snowmelt runoff in historical baseline estimates increased up to elevations of 3600–3800 m (gradient

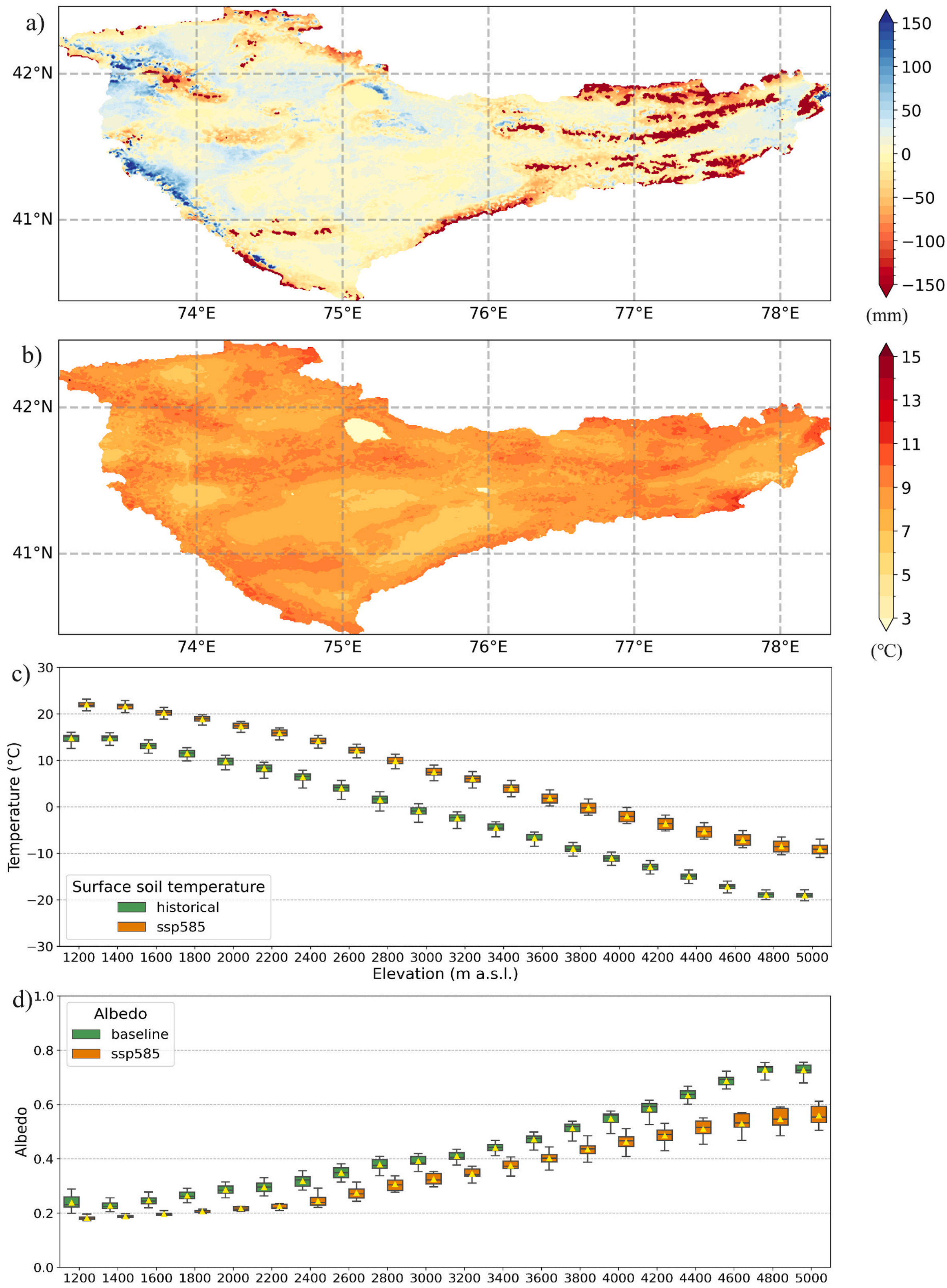

Fig. 6. Differences between base period (1981–2000) and future projections (2077–2096) in Naryn River basin for a) total runoff depth b) surface soil temperature, c) surface soil temperature and d) albedo at different elevations across the basin.

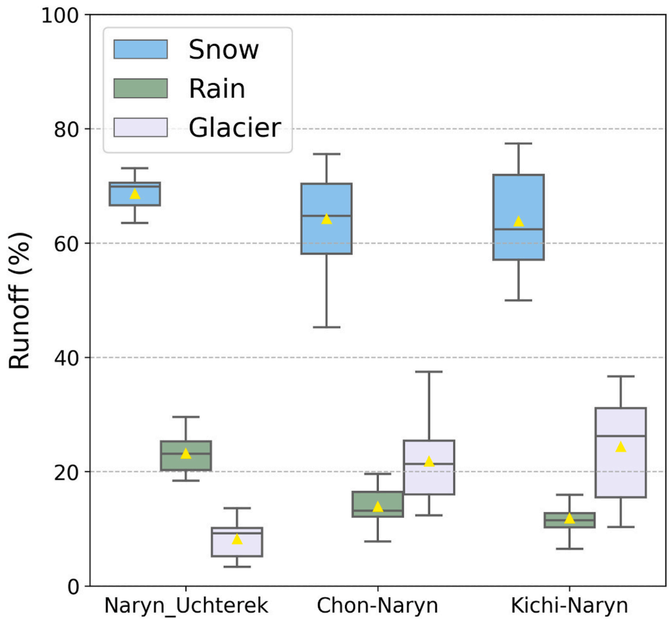

Fig. 7. Contribution variations of snow, rain and glacier components across the study basins for the base period (1981–2000).

of 27 mm/100m). The maximum peak snowmelt runoff was estimated at elevations of 3800 m for the baseline period with an average value of 470 mm, indicating large accumulations of snow in this altitude zone followed by subsequent melt during warmer periods (Fig. 8c). After reaching the peak, snowmelt runoff gradually decreased exhibiting accumulation at the highest elevations.

In the climate change scenario, there is a noticeable trend of decreasing snowmelt runoff up to an elevation of 4000 m (the current snow line zone) compared to baseline period, followed by an increase in runoff at higher elevations (Fig. 8c). The gradient of snowmelt runoff for elevation ranges from 2200 m to 3600 m remains consistent at 26 mm/100 m, almost matching baseline estimates. The decrease in snowmelt runoff within the elevation range of up to 4000 m indicates that there may be less water available and a reduced capacity to retain water in warmer seasons. However, the zone of largest snowmelt contributions shifts to higher elevations (above 4000 m Fig. 8c) in the climate projections, indicating the potential for increased seasonal runoff. The overall projected reduction in snowmelt runoff for the entire Naryn River basin is 12%, offset by the compensating effects of higher elevation zones.

To estimate total runoff, all sources and components of the water balance (except permafrost) were considered, including rainfall runoff, snowmelt runoff, glaciermelt runoff, surface evaporation, snow and glacier sublimation, and transpiration (Fig. 8d). The trend of increasing runoff with elevation is particularly apparent at elevations from 2000 to 3600 m, ranging from 93 mm to 402 mm, respectively (Fig. 8d). Above

Table 1
Meteorological forcing and land data used in this study.

Variable	Unit	Resolution	Source
Wind speed	m s^{-1}	0.04° × 0.04°, hourly	NHRCM-CA (Isaev et al., 2024)
SW downward radiation	W m^{-2}		
LW downward radiation	W m^{-2}		
Surface air pressure	Pa		
Specific humidity	kg/kg		
2 m temperature	K		
Precipitation	mm		
Land cover		1 km	GLCC ver2.0 (Loveland et al., 2000)
Glacier cover		100 m	Randolph Glacier Inventory (RGI) version 6.0 (RGI-Consortium, 2017)
Surface parameters		1 km	Ecoclimap (Champeaux et al., 2005)

Abbreviations: SW – shortwave, LW – longwave.

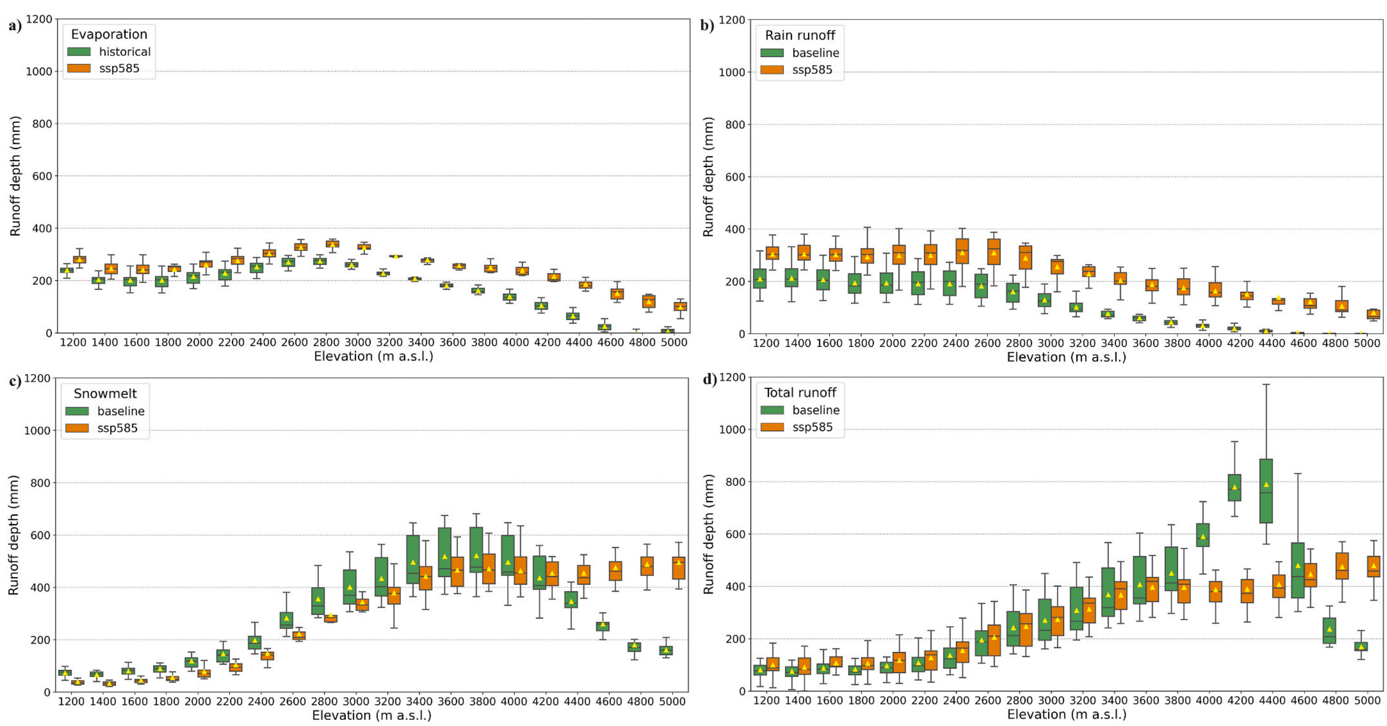

Fig. 8. Comparison of runoff components between the base period (1981–2000) and future projections (2077–2096) for a) evaporation b) rain runoff c) snowmelt runoff and d) total runoff at different elevations across the Naryn River basin.

this zone, a significant contribution from glaciermelt runoff is observed, followed by a gradual decrease in runoff towards minimum values at the highest elevations. Variability of total runoff differed by elevation. Higher elevation zones, especially glaciated areas, had very high variability (Figs. 8 and 9), indicating a potentially compensating effect of runoff from these zones in response to snowfall variability.

When comparing changes in total baseline runoff with the climate scenario in the case of complete glacier degradation due to higher temperatures in lower zones, liquid precipitation runoff will dominate and, even with increased evaporation, overall runoff will increase due to the increased precipitation trends in lower zones. Noteworthy is that the previous rain to snow ratio of 3:1 will shift to 3:2.35. In the transitional zone (≈2500–3500 m), a decline in mean total runoff occurs attributed to the transition from snow to rain and intense evaporation. However, median values are elevated, and overall variability is reduced compared to the baseline period. Above this zone, there is a projected reduction in total runoff – e.g., at 4200 m, there is a 51% reduction in total runoff primarily due to the disappearance of glaciers. However, in the accumulation zone above 4600 m, we observe a relative increase in runoff due to the melting of snow, which previously accumulated and served as a source for glaciers.

3.4. Total runoff standardized anomaly index

The high variability of water balance components in glaciated basins represents a highly sensitive system for seasonal water supplies. Analysis of the Total Runoff Standardized Anomaly Index (TR-SAI) by year reveals substantial variability in the distribution of water availability across the basin (Fig. 9). However, a clear overall trend is observed in the elevation distribution of the index. For instance, increased TR-SAI is observed throughout the Naryn River basin area in 1992 (Fig. 9a) due to a higher amount of precipitation in the basin (Fig. S5c). In contrast, in high mountainous regions, particularly in glacier formation zones, the TR-SAI index is negative, possibly attributed to a delay in the onset of glacier melt due to the presence of large seasonal snowpacks on glaciers that result in a negative anomaly in the water balance index for these

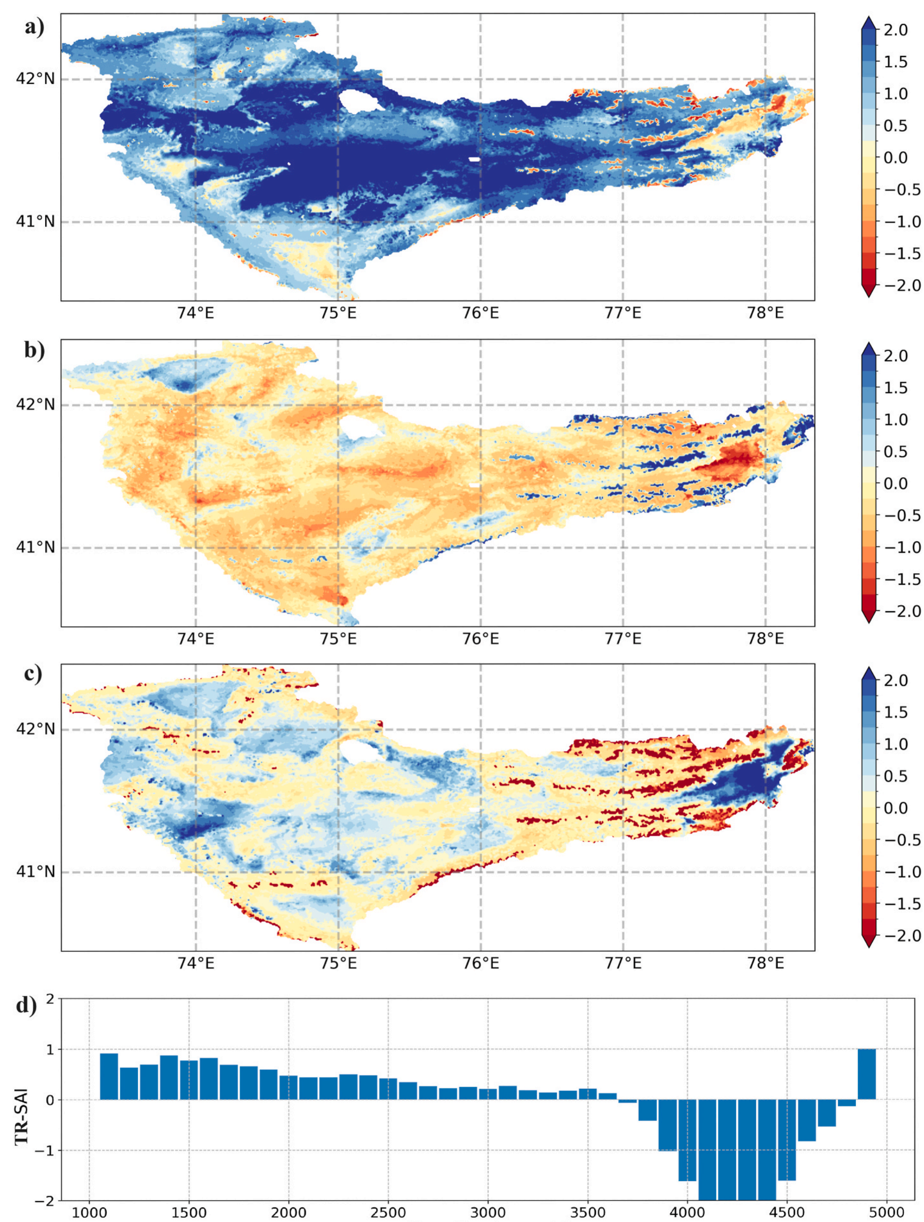

Fig. 9. Calculated Total Runoff Standardized Anomaly Index (TR-SAI) for a) wet year in 1992; b) dry year in 1993; c) mean index difference for future projections; and d) index difference for future projections across elevations.

high-altitude zones.

The modeled runoff source distributions (Fig. S5) clearly illustrate distinct patterns within the basin. In 1993, the basin experienced relative aridity, indicated by a negative TR-SAI (Fig. 9b). Conversely, the glacierized areas in the upper basin displayed extreme TR-SAI values, suggesting a significant contribution of runoff from glacier melt for that period. This compensatory effect offset the reduced runoff caused by weak precipitation accumulation. The TR-SAI serves as a useful indicator of the importance of glaciers in generating runoff from precipitation, both spatially and temporally. Additionally, it reveals potential changes in this relationship under the SSP5-8.5 climate scenario.

The analysis of this index based on a historical baseline simulation provides insights into the potential variability of annual conditions across the entire region under future climate scenarios (Fig. 9c). The findings are intriguing, revealing high spatial heterogeneity in TR-SAI patterns. Notably, in the upper Naryn basin, where the river originates

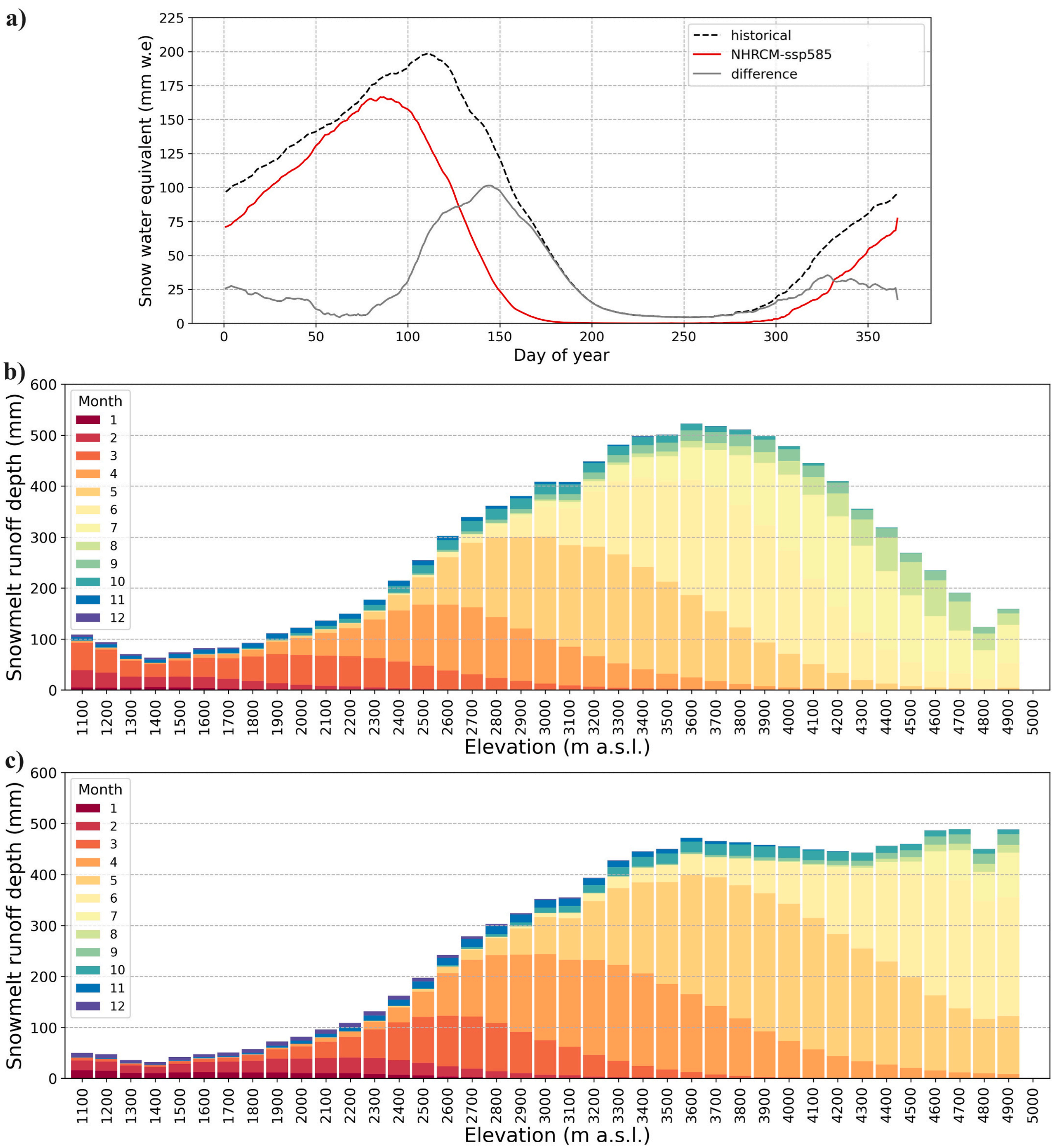

Fig. 10. Changes of basin mean snow water equivalent and snowmelt runoff: a) comparison of seasonal SWE changes between the historical baseline period and future SSP5-8.5 projections b) seasonal snowmelt runoff distribution across elevations for baseline and c) future projections.

from a plateau above 3000 m (excluding glaciers), a significant increase in total runoff variation is observed. This phenomenon becomes apparent when comparing the changes in average surface runoff (Fig. 6a).

Furthermore, a clear elevation-based pattern emerges when examining the variability of the TR-SAI index (Fig. 9d). Lower-lying regions from 1000 m exhibit higher index values, which gradually decrease with increasing elevation up to 3500 m (prior to the glacier formation zone). This trend indicates a pronounced positive variability in runoff generation. Considering the previously identified changes in temperature affecting the upper soil layer, it can be inferred that increased evaporation will have substantial implications for the water balance of the region, particularly in the upper reaches of the basin.

3.5. Snow water equivalent changes

Our analysis examined the changes in snow water equivalent (SWE) using the regional model for both historical baseline and future scenarios (Fig. 10a). For the baseline period from 1981 to 2000, we observed that the peak of snow accumulation, typically in the second half of April (Julian day 115) with approximately 200 mm of SWE, was shifted by 26 days to the end of March. This indicates a shift in the timing of peak snow accumulation due to increased temperatures and reduced snowfall. Furthermore, the maximum changes relative to the baseline scenario were observed during the peak of snowmelt in May (Julian day 145). During this period, the maximum change in SWE was 100 mm, indicating a likely decrease in water runoff from snowmelt. On average, a reduction of 17% in peak values of SWE compared to baseline levels were observed.

Elevational and seasonal patterns of snowmelt runoff were compared between historical baseline (Fig. 10b) and future (Fig. 10c) scenarios. At lower elevations, significant reductions in runoff are projected from February to April, attributed to the limited availability of snow during this period. The snowmelt pattern in April under the future scenario closely resembles the historical pattern observed in March, indicating an earlier onset of snowmelt. However, a larger proportion of the snowpack water will be released in April–May rather than the baseline May–June timeframe.

In the historical baseline simulation (Fig. 10b), peak snowmelt volume occurred at elevations between 3300 m and 4000 m. Conversely, under climate change conditions, the accumulation zones will play a more significant role in the water balance causing the peak snowmelt volume to shift to higher elevations (above 4000 m) and become dependent on the overall precipitation volume.

Notably, snowmelt volumes in July and August are projected to decline substantially, exposing glacier surfaces much earlier and potentially accelerating the melting of remaining glaciers. This trend is evident in the mean seasonal snow water equivalent (Fig. 10a), which indicates a near-absence of snow cover during the July–August period.

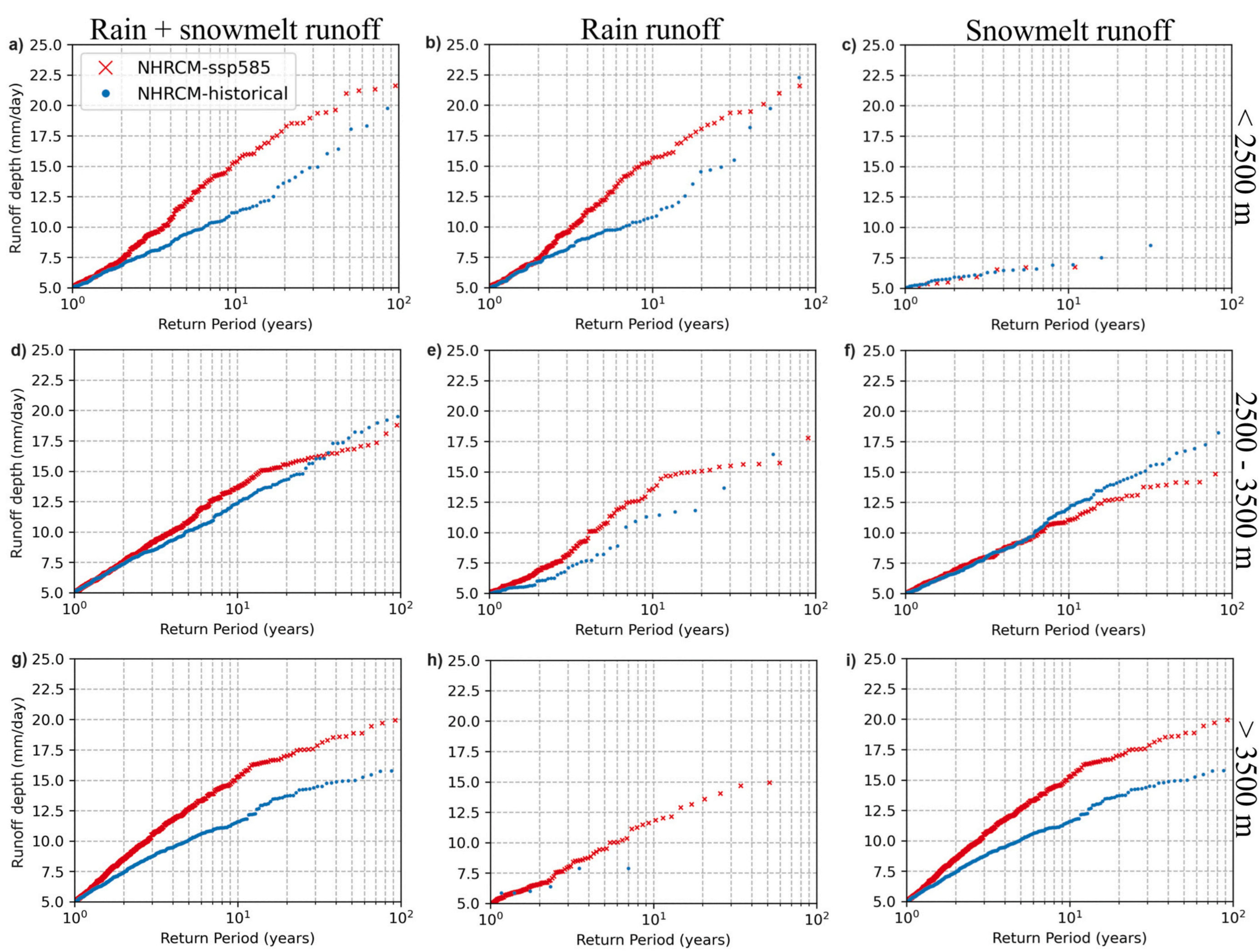

Fig. 11. Comparison of extreme daily runoff between the historical baseline period and SSP5-8.5 projections for total of rainfall and snowmelt runoff (a,d,g), rainfall runoff (b,e,h) and snowmelt runoff (c,f,i) at different elevations zones: <2500m (a,b,c), 2500–3500m (d,e,f) and >3500m (g,h,i).

3.6. Changes in extreme runoff

When comparing data on extreme runoff in the Naryn River basin, considering the worst-case climate change scenario SSP5-8.5, several future patterns emerge (Fig. 11). Below 2500 m, the primary source of extreme runoff is rainfall, while melting of snowpacks has minimal influence due to limited accumulation at these elevations (Fig. 11a–c). For the climate change scenario, the impact of snowmelt will be even less significant. In terms of rainfall runoff, there is a projected increase in runoff depth intensity, particularly for the 5, 10, and 20-year return periods, with increases of 27%, 44%, and 24% respectively. Additionally, 10-year maximum runoff events derived from baseline estimations are projected to occur every 3–4 years by the end of the 21st Century.

At altitudes from 2500 m to 3500 m (Fig. 11d–f), where the transition of precipitation between rain and snow is important, we see that despite the increases in overall maximum runoff from snowmelt and rainfall (average increase of 8.6% for the 5, 10, and 20-year periods) this increase is attributed to intensified rainfall runoff at these altitudes due to rising temperatures. However, the intensity of snowmelt runoff declined by an average of 10.8% due to the reduction in the total snow cover across these elevations throughout the basin.

For altitudes above 3500 m (Fig. 11g–i), where snowmelt is the primary source of runoff, intense rainfall events will occur more frequently with climate change. However, their magnitude will not surpass the contribution from snowmelt. On average, the intensity of maximum snowmelt runoff for these altitudes will increase by 26.5% for all return periods, which can be attributed to the overall trend of accelerated melting due to increased energy for snowpack ripening and amount of solid precipitation.

4. Discussion

The persistent mismatch in scales between hydrological and atmospheric models underscores the critical need for grid-scale land surface hydrological models that can better resolve the complex, nonlinear interactions with atmospheric processes at spatial resolutions required for robust climate impact assessments (Hostetler, 1994). Nested regional climate models, which dynamically downscale global climate model outputs to finer spatial scales, offer a promising approach to bridge the scale gap and more accurately capture the regional-scale hydrological responses to climate change (Teutschbein and Seibert, 2010). Continued advancements in the integration and coupling of grid-scale land surface hydrological models within nested regional climate modeling frameworks hold great potential for developing the next generation of climate change impact assessment tools that can robustly address the challenge of discordant scales across the hydrosphere-atmosphere system.

Our results of the main characteristics and changes in the Naryn River basin closely align with previous studies. The overall historical baseline glacier melt contribution of 7% was quite close to the 6% simulated using the SWAT model (Gan et al., 2015). For the upper basins, the average values were 22% and 24%, which coincides with Saks et al. (2022) average findings of 23%. Additionally, assessments of glacier melt contributions using remote sensing methods yielded 30.7% and 23.9% for Chon-Naryn and Kichi-Naryn basins, respectively. A notable difference is that even under the worst-case SSP5-8.5 scenario, in the condition of total glacier degradation, the reduction in total streamflow would be 16% (Table 2), which also matches the 17% decrease reported by Gan et al. (2015), despite about 35% of the original glacier area remaining in Gan et al.'s study. This highlights the significant impact of glacier retreat and additional runoff sourced from previously accumulated snow at higher elevations on basin hydrology with increases in precipitation sourced runoff of 17% (80 mm yr^{-1}) and overall increases in precipitation of 14%. However, a more substantial divergence was observed in the estimated changes in evapotranspiration. While previous modeling efforts had indicated a 9% increase (Gan et al., 2015), our study found a much higher increase (33%; Table 2). This discrepancy suggests the need for further investigation into the drivers and processes governing evapotranspiration in the Naryn River basin under climate change conditions as higher altitudes will be extensively exposed to positive temperatures and increased water availability due to temporally shifted snowmelt.

Modeling evapotranspiration is a significant challenge in assessing climate change, with significant variations in methodologies and approaches (Kay and Davies, 2008; Kingston et al., 2009; Barella-Ortiz et al., 2013; Abiodun et al., 2018). In our study, the actual evapotranspiration is highly dependent on the presence of moisture and shifts in the energy balance. Especially at mid-elevations, we observe a peak in evapotranspiration, similar to studies conducted in other mountainous regions, with a potential forecast of a 28% increase by the year 2100 (Goulden and Bales, 2014). In cryosphere zones, evapotranspiration is expected to increase more significantly compared to other areas, with boreal needleleaf deciduous forests (decadal mean: 309 mm yr^{-1}) and tundra (200 mm yr^{-1}) experiencing the largest increases of 32.7% and 26.6%, respectively (Pan et al., 2015). Snow water equivalent changes suggest a corresponding increase in available energy for evapotranspiration, especially at higher elevations where snow cover will rapidly decrease and shifts from snow to rain provide additional moisture for evaporation, highlighting the role of the snow/ice albedo feedback in shaping future climate change patterns in mountainous regions (Arakawa, 2012; Pepin et al., 2015). It is evident from Fig. 6a that changes in total runoff will predominantly affect the upper basins of Chon-Naryn and Kichi-Naryn creating vulnerable post-glacial ecosystems in these catchments (Bosson et al., 2023).

A significant contrast between temperatures at higher and lower altitudes is particularly evident during the summer and autumn months (Fig. 4a). Increased precipitation is projected in the eastern part of the basin (Fig. 3b), specifically in Chon-Naryn and Kichi-Naryn. This anomaly may be attributed to the influence of Issyk-Kul lake located to the north of these basins, which experiences intense evaporation in summer (Romanovsky et al., 2013), possibly exerting an impact on the mass balance of glaciers in that area (Van Tricht et al., 2021). Noteworthy, is that global climate models and low-resolution regional models may not fully account for evaporation from water bodies (Erler et al., 2019; Teutschbein and Seibert, 2012), whereas the non-hydrostatic model utilized in our study offers a more accurate depiction of moisture transport within the region. It is indeed a delicate balance in modeling the interactions among atmosphere, hydrosphere, and cryosphere components when assessing potential changes in

Table 2
Changes in runoff composition of the study basins (*glaciers are excluded for the future scenario, hist – historical baseline period 1981–2000, ssp585 – future climate scenario period 2077–2096).

	Naryn (Toktogul inflow)			Chon-Naryn			Kichi-Naryn		
Variable (mm yr^{-1})	**hist**	**ssp585**	**%**	**hist**	**ssp585**	**%**	**Hist**	**ssp585**	**%**
Total runoff	250	209	−16	268	157	−41	441	254	−42
Rain runoff	121	244	+102	65	221	+240	79	224	+184
Snowmelt	357	314	−12	305	262	−14	426	366	−14
Glacier melt*	41	0	−100	102	0	−100	159	0	−100
Evaporation	226	301	+33	176	303	+72	181	304	+68

processes that determine the future state of ecosystems.

An important yet understudied aspect is the influence of changes in runoff during extreme events in mountainous regions such as floods, landslides, and debris flows (Ingold et al., 2010; Beniston and Stoffel, 2014). Such changes need to be assessed considering the transition from snow to rain, the intensity of snowmelt, and the spatial distribution of this phenomenon (Harpold and Kohler, 2017). As observed from our modeling results, the lower regions will primarily be susceptible to extreme runoff due to an increase in the rainfall fraction, its quantity, and frequency. On the other hand, the upper basin will experience extremes due to intensified snowmelt, which may amplify the impact of rain-on-snow floods (Ombadi et al., 2023). The transition from a snow-dominated to a rain-dominated hydrological regime can lead to earlier and more intense peak flows, increased flood risk in lower elevations, and a heightened potential for rain-on-snow events (Cohen et al., 2015) that can trigger destructive debris flows and landslides in the upper catchments. Understanding these complex interactions among changes in precipitation phase, snowpack dynamics, and the generation of extreme events is essential for developing effective adaptation strategies and risk management plans in mountainous regions.

Regarding the uncertainties, the methodology previously evaluated under similar conditions using stationary observations, including the energy balance, suggests that the main factor of uncertainty is the input meteorological data (Sadyrov et al., 2024). There might be uncertainties arising from the mismatch between the scale of observations (point measurements) and the scale of model grid cells, particularly in areas with high spatial heterogeneity. The complexity lies in the fact that most of the weather stations used to validate the regional climate model are located in lowlands, and only one is located above 3000 m (Fig. 1). Indeed, extensive observations of the cryosphere and atmospheric data in the region have been very inefficient, although additional support is gradually improving the situation (Hoelzle et al., 2017). The results indicate a certain overestimation of precipitation in the mountainous areas, which is also evident from the analysis of the water balance components, especially in the Kichi-Naryn basin (Fig. S5).

There are many key advantages of the high-resolution modeling approach employed in this study and these offer significant improvements over previous coarser-scale assessments. By utilizing a fully distributed (1 km) land surface and glaciological model, it was possible to capture the fine-scale variations in topography, land cover, and climate factors within the Naryn River basin, providing a more accurate depiction of the spatial distribution of runoff sources, evapotranspiration processes, and other energy and water balance components – a crucial advantage in mountainous, glacierized basins where cryospheric components are major drivers of the water cycle and exhibit substantial heterogeneity across the landscape. The high-resolution regional climate model (5 km) also offered more reliable meteorological forcing data, improving the representation of local climate variations and the simulation of future changes, while the physically-based nature of the models reduced the need for extensive calibration, allowing for broader application beyond the Naryn basin. Although the overall findings may be consistent with previous studies, the high-resolution approach in this work offers a more robust and spatially explicit understanding of the complex hydrological processes and their responses to climate change in the Naryn River basin, which is essential for informing effective water resources management and adaptation strategies in this water-stressed region of Central Asia.

5. Conclusion

The study presents a comprehensive assessment of the potential impacts of climate change on the surface energy and water balance in the Naryn River basin, a crucial catchment in Central Asia supplying water to four nations. The region is highly dependent on glaciers and snowmelt, which are being significantly affected by climate change, including rising temperatures and altered precipitation patterns.

To conduct this assessment, we employed high-resolution (5 km) regional climate projections that were validated for the Central Asia region. These climate data were then used to drive a fully distributed (1 km) land surface and glaciological energy-mass balance model. The study compared historical baseline simulations from 1981 to 2000 with future projections for 2077–2096 under the worst-case SSP5-8.5 climate change scenario, considering the complete degradation of glaciers by the end of the century. The results show that with the complete loss of glaciers and a consequent 33% increase in evapotranspiration, the overall runoff in the Naryn River basin will decrease by 16%, with reductions exceeding 40% in upper basins. The snow-albedo feedback effect could potentially drive an increase in soil surface temperature, with a gradient of 0.1 °C per 100 m elevation, leading to a projected increase of 10.4 °C at higher elevations. The maximum snow water equivalent (SWE) is projected to decrease by 17%, with the seasonal peak occurring one month earlier, exposing earlier glacier melt and disrupting the pattern of glacier accumulation. Furthermore, the transition from snow to rain will significantly impact the lower basin, increasing peak runoff and causing 10-year recurrence interval events to occur every 3–4 years. Conversely, extreme runoff in the high mountainous areas is projected to increase due to intensified snowmelt, more snow and increased rainfall extremes.

Simulations using advanced physical models can accurately depict significant changes in the hydrological components of a given basin. Additionally, input data in the form of climate projections generated by high-resolution regional climate models can provide a more comprehensive understanding of future changes. Noteworthy is that this approach requires minimal calibration and primarily relies on meteorological inputs, which can be enhanced through bias corrections. This is a significant advantage, as it enables the exploration of hydrological changes at broader spatial scales, going beyond the constraints of individual basins. This expands the inference of this approach to assessment of the homogeneity of parameters for its application in other regional studies. However, the accuracy of these model-derived projections may be compromised by the limited availability of observational data, especially in topographically complex regions where weather station coverage is sparse.

CRediT authorship contribution statement

Sanjar Sadyrov: Writing – original draft, Visualization, Validation, Methodology, Investigation, Formal analysis, Data curation, Conceptualization. **Erkin Isaev:** Writing – review & editing, Visualization, Methodology, Investigation, Formal analysis, Data curation. **Kenji Tanaka:** Writing – review & editing, Supervision, Project administration, Methodology, Formal analysis. **Akihiko Murata:** Writing – review & editing, Project administration, Data curation. **Roy C. Sidle:** Writing – review & editing, Supervision, Project administration.

Declaration of competing interest

The authors declare that they have no known competing financial interests or personal relationships that could have appeared to influence the work reported in this paper.

Acknowledgements

We would like to express our sincere gratitude to the Meteorological Research Institute of Japan for providing the high-resolution climate forcing data over Central Asia. This dataset was developed with support from the MEXT-Program for the Advanced Studies of Climate Change Projection (SENTAN) under Grant Number JPMXD0722680734.

Appendix A. Supplementary data

Supplementary data to this article can be found online at https://doi.

org/10.1016/j.jenvman.2024.124021.

Data availability

Data will be made available on request.

References

Abiodun, O.O., Guan, H., Post, V.E., Batelaan, O., 2018. Comparison of MODIS and SWAT evapotranspiration over a complex terrain at different spatial scales. Hydrol. Earth Syst. Sci. 22 (5), 2775–2794.

Aizen, V., Aizen, E., 1997. Hydrological cycles on the north and south peripheries of mountain–glacial basins of Central Asia. Hydrol. Process. 11 (5), 451–469.

Aizen, V.B., Aizen, E.M., Melack, J.M., 1995. Climate, snow cover, glaciers, and runoff in the tien Shan, central asia. JAWRA J. Am. Water Resour. Assoc. 31. https://doi.org/10.1111/j.1752-1688.1995.tb03426.x.

Arakawa, O., 2012. Elevation dependency of summertime precipitation and its change by global warming over the Tibetan plateau and the surroundings simulated by a 60-km-mesh atmospheric general circulation model. Journal of the Meteorological Society of Japan. Ser. II 90A (0), 151–165. https://doi.org/10.2151/jmsj.2012-a08.

Bai, P., Liu, X., Liang, K., Liu, C., 2015. Comparison of performance of twelve monthly water balance models in different climatic catchments of China. J. Hydrol. 529 (3), 1030–1040. https://doi.org/10.1016/j.jhydrol.2015.09.015.

Bai, P., Liu, X., Liu, C., 2018. Improving hydrological simulations by incorporating GRACE data for model calibration. J. Hydrol. 557, 291–304.

Barandun, M., Pohl, E., 2023. Central Asia's spatiotemporal glacier response ambiguity due to data inconsistencies and regional simplifications. Cryosphere 17 (3), 1343–1371.

Barandun, M., Fiddes, J., Scherler, M., Mathys, T., Saks, T., Petrakov, D., Hoelzle, M., 2020. The state and future of the cryosphere in Central Asia. Water Security 11, 100072.

Barella-Ortiz, A., Polcher, J., Tuzet, A., Laval, K., 2013. Potential evaporation estimation through an unstressed surface-energy balance and its sensitivity to climate change. Hydrol. Earth Syst. Sci. 17 (11), 4625–4639.

Barron, O., Silberstein, R., Ali, R., Donohue, R., McFarlane, D.J., Davies, P., Hodgson, G., Smart, N., Donn, M., 2012. Climate change effects on water-dependent ecosystems in south-western Australia. J. Hydrol. 434–435, 95–109. https://doi.org/10.1016/j.jhydrol.2012.02.028.

Beniston, M., Stoffel, M., 2014. Assessing the impacts of climatic change on mountain water resources. Sci. Total Environ. 493, 1129–1137.

Beven, K., 2006. A manifesto for the equifinality thesis. J. Hydrol. 320 (1–2), 18–36.

Beven, K., Freer, J., 2001. Equifinality, data assimilation, and uncertainty estimation in mechanistic modelling of complex environmental systems using the GLUE methodology. J. Hydrol. 249 (1–4), 11–29.

Bosson, J.B., Huss, M., Cauvy-Fraunié, S., Clément, J.C., Costes, G., Fischer, M., et al., 2023. Future emergence of new ecosystems caused by glacial retreat. Nature 620 (7974), 562–569.

Cao, L., Xu, C., Suo, N., Song, L., Lei, X., 2023. Future dry-wet climatic characteristics and drought trends over arid central asia. Front. Earth Sci. 11. https://doi.org/10.3389/feart.2023.1102633.

Carletti, F., Michel, A., Casale, F., Burri, A., Bocchiola, D., Bavay, M., Lehning, M., 2022. A comparison of hydrological models with different level of complexity in Alpine regions in the context of climate change. Hydrol. Earth Syst. Sci. 26 (13), 3447–3475.

Champeaux, J.L., Masson, V., Chauvin, F., 2005. ECOCLIMAP: a global database of land surface parameters at 1 km resolution. Meteorol. Appl.: A journal of forecasting, practical applications, training techniques and modelling 12 (1), 29–32.

Chang, S., Isaev, E., Chen, H., Wu, B., Meng, J., Yan, N., Ma, Z., 2024. Exploring the linkages between different types of drought and their impacts on crop production in Kyrgyzstan. IEEE J. Sel. Top. Appl. Earth Obs. Rem. Sens. https://doi.org/10.1109/JSTARS.2024.3359429.

Chen, Y., Li, W., Deng, H., Fang, G., Li, B., 2016. Changes in central asia's water tower: past, present and future. Sci. Rep. 6 (1). https://doi.org/10.1038/srep35458.

Chen, Y., Li, W., Fang, G., Li, Z., 2017. Hydrological modeling in glacierized catchments of central Asia–status and challenges. Hydrol. Earth Syst. Sci. 21 (2), 669–684.

Cohen, J., Ye, H., Jones, J., 2015. Trends and variability in rain-on-snow events. Geophys. Res. Lett. 42 (17), 7115–7122.

Coron, L., Andreassian, V., Perrin, C., Lerat, J., Vaze, J., Bourqui, M., Hendrickx, F., 2012. Crash testing hydrological models in contrasted climate conditions: an experiment on 216 Australian catchments. Water Resour. Res. 48 (5).

Cosby, B.J., Hornberger, G.M., Clapp, R.B., Ginn, T., 1984. A statistical exploration of the relationships of soil moisture characteristics to the physical properties of soils. Water Resour. Res. 20 (6), 682–690.

Erler, A.R., Frey, S.K., Khader, O., d'Orgeville, M., Park, Y.J., Hwang, H.T., et al., 2019. Simulating climate change impacts on surface water resources within a lake-affected region using regional climate projections. Water Resour. Res. 55 (1), 130–155.

Farinotti, D., Longuevergne, L., Moholdt, G., Duethmann, D., Mölg, T., Bolch, T., et al., 2015. Substantial glacier mass loss in the Tien Shan over the past 50 years. Nat. Geosci. 8 (9), 716–722.

Fowler, K.J.A., Peel, M.C., Western, A.W., Zhang, L., Peterson, T.J., 2016. Simulating runoff under changing climatic conditions: revisiting an apparent deficiency of conceptual rainfall-runoff models. Water Resour. Res. 52 (3), 1820–1846. https://doi.org/10.1002/2015wr018068.

Fujita, K., Ageta, Y., 2000. Effect of summer accumulation on glacier mass balance on the Tibetan Plateau revealed by mass-balance model. J. Glaciol. 46, 244–252. https://doi.org/10.3189/172756500781832945.

Fujita, K., Sakai, A., 2014. Modelling runoff from a Himalayan debris-covered glacier. Hydrol. Earth Syst. Sci. 18, 2679–2694. https://doi.org/10.5194/hess-18-2679-2014.

Fujita, K., Takeuchi, N., Nikitin, S.A., Surazakov, A.B., Okamoto, S., Aizen, V.B., Kubota, J., 2011. Favorable climatic regime for maintaining the present-day geometry of the Gregoriev Glacier, Innerinner Tien Shan. Cryosphere 5, 539–549.

Gan, R., Luo, Y., Zuo, Q., Sun, L., 2015. Effects of projected climate change on the glacier and runoff generation in the Naryn River Basin, Central Asia. J. Hydrol. 523, 240–251.

Goulden, M.L., Bales, R.C., 2014. Mountain runoff vulnerability to increased evapotranspiration with vegetation expansion. Proc. Natl. Acad. Sci. USA 111 (39), 14071–14075.

Harpold, A.A., Kohler, M., 2017. Potential for changing extreme snowmelt and rainfall events in the mountains of the western United States. J. Geophys. Res. Atmos. 122 (24), 13–219.

Hasson, S., Lucarini, V., Pascale, S., Böhner, J., 2014. Seasonality of the hydrological cycle in major South and Southeast Asian river basins as simulated by PCMDI/CMIP3 experiments. Earth System Dynamics 5 (1), 67–87. https://doi.org/10.5194/esd-5-67-2014.

Her, Y., Yoo, S.H., Cho, J., Hwang, S., Jeong, J., Seong, C., 2019. Uncertainty in hydrological analysis of climate change: multi-parameter vs. multi-GCM ensemble predictions. Sci. Rep. 9 (1), 4974.

Hill, A.F., Minbaeva, C.K., Wilson, A.M., Satylkanov, R., 2017. Hydrologic controls and water vulnerabilities in the Naryn River Basin, Kyrgyzstan: a socio-hydro case study of water stressors in Central Asia. Water 9 (5), 325.

Hoelzle, M., Azisov, E., Barandun, M., Huss, M., Farinotti, D., Gafurov, A., et al., 2017. Re-establishing glacier monitoring in Kyrgyzstan and Uzbekistan, Central Asia. Geoscientific Instrumentation, Methods and Data Systems 6 (2), 397–418.

Hostetler, S.W., 1994. Hydrologic and atmospheric models: the (continuing) problem of discordant scales: an Editorial Comment. Climatic Change 27 (4), 345–350. https://doi.org/10.1007/BF01096266.

Huss, M., Hock, R., 2018. Global-scale hydrological response to future glacier mass loss. Nat. Clim. Change 8 (2), 135–140.

Ingold, K., Balsiger, J., Hirschi, C., 2010. Climate change in mountain regions: how local communities adapt to extreme events. Local Environ. 15 (7), 651–661.

Isaev, E., Murata, A., Fukui, S., Sidle, R.C., 2024. High-resolution dynamic downscaling of historical and future climate projections over Central Asia. Central Asian J Water Res 10 (1).

Kalashnikova, O.Y., Niyazov, J., Nurbatsina, A., Kodirov, S., Radchenko, Y., Kretova, Z., 2023. Kyrgyz transboundary rivers' runoff assessment (Syr-darya and Amu-darya river basins) in climate change scenarios. Central Asian J Water Res 9, 59–88.

Kay, A.L., Davies, H.N., 2008. Calculating potential evaporation from climate model data: a source of uncertainty for hydrological climate change impacts. J. Hydrol. 358 (3–4), 221–239.

Kingston, D.G., Todd, M.C., Taylor, R.G., Thompson, J.R., Arnell, N.W., 2009. Uncertainty in the estimation of potential evapotranspiration under climate change. Geophys. Res. Lett. 36 (20).

Kondo, J., Xu, J., 1997. Seasonal variations in the heat and water balances for nonvegetated surfaces. J. Appl. Meteorol. 36, 1676–1695.

Kriegel, D., Mayer, C., Hagg, W., Vorogushyn, S., Duethmann, D., Gafurov, A., Farinotti, D., 2013. Changes in glacierisation, climate and runoff in the second half of the 20th century in the Naryn basin, Central Asia. Global Planet. Change 110, 51–61.

Loveland, T.R., Reed, B.C., Brown, J.F., Ohlen, D.O., Zhu, Z., Yang, L.W.M.J., Merchant, J.W., 2000. Development of a global land cover characteristics database and IGBP DISCover from 1 km AVHRR data. Int. J. Rem. Sens. 21 (6–7), 1303–1330.

McKee, T.B., Doesken, N.J., Kleist, J., 1993. The relationship of drought frequency and duration to time scales. In: Proceedings of the 8th Conference on Applied Climatology, 17, pp. 179–183, 22.

Niu, G.-Y., Yang, Z.-L., 2007. An observation-based formulation of snow cover fraction and its evaluation over large North American river basins. J. Geophys. Res. Atmos. 112. https://doi.org/10.1029/2007JD008674.

Nuimura, T., Sakai, A., Taniguchi, K., Nagai, H., Lamsal, D., Tsutaki, S., Kozawa, A., Hoshina, Y., Takenaka, S., Omiya, S., 2015. The GAMDAM glacier inventory: a quality-controlled inventory of Asian glaciers. Cryosphere 9, 849–864.

Ombadi, M., Risser, M.D., Rhoades, A.M., Varadharajan, C., 2023. A warming-induced reduction in snow fraction amplifies rainfall extremes. Nature 619 (7969), 305–310.

Pan, S., Tian, H., Dangal, S.R., Yang, Q., Yang, J., Lu, C., et al., 2015. Responses of global terrestrial evapotranspiration to climate change and increasing atmospheric CO2 in the 21st century. Earth's Future 3 (1), 15–35.

Park, S., Lim, C.H., Kim, S.J., Isaev, E., Choi, S.E., Lee, S.D., Lee, W.K., 2021. Assessing climate change impact on cropland suitability in Kyrgyzstan: where are potential high-quality cropland and the way to the future. Agronomy 11 (8). https://doi.org/10.3390/AGRONOMY11081490.

Pepin, N., Bradley, R.S., Diaz, H.F., Baraer, M., Caceres, E.B., Forsythe, N., Fowler, H., Greenwood, G., Hashmi, M.Z., Liu, X.D., Miller, J.R., Ning, L., Ohmura, A., Palazzi, E., Rangwala, I., Schöner, W., Severskiy, I., Shahgedanova, M., Wang, M.B., Williamson, S.N., Yang, D.Q., 2015. Elevationdependent warming in mountain regions of the world. Nat. Clim. Change 5, 424–430. https://doi.org/10.1038/NCLIMATE2563.

Seiller, G., Anctil, F., Perrin, C., 2012. Multimodel evaluation of twenty lumped hydrological models under contrasted climate conditions. Hydrol. Earth Syst. Sci. 16 (4), 1171, 1189.

Petrakov, D., Tutubalina, O., Shpuntova, A., Kovalenko, N., Usubaliev, R., Azisov, E., Mikhailukova, P., 2019. Assessment of glacier albedo in the Ak-Shyirak mountains (inner Tien Shan) from ground-based and Landsat data. Earths Cryosphere XXIII, 13–24. https://doi.org/10.21782/KZ1560-7496-2019-3(13-24.
Podrezov, O., 2001. Izmenchivost'Klimaticheskikh usloviy I oledeneniya tyan-shanya za poslednie 100 let.(variability of the climatic conditions and the glaciation of tien Shan during the past 100 years). Vestnik: KRSU 33–40.
Pohl, E., Gloaguen, R., Andermann, C., Knoche, M., 2017. Glacier melt buffers river runoff in the Pamir Mountains. Water Resour. Res. 53 (3), 2467–2489.
Pritchard, H.D., 2017. Asia's glaciers are a regionally important buffer against drought. Nature 545 (7653), 169–174.
Radchenko, I., Forkutsa, I., Frede, H., 2014. Simulating water resource availability under data scarcity—a case study for the ferghana valley (central asia). Water 6 (11), 3270–3299. https://doi.org/10.3390/w6113270.
RGI-Consortium, 2017. Randolph Glacier Inventory–A Dataset of Global Glacier Outlines: Version 6.0: Technical Report, Global Land Ice Measurements From Space. Digital Media, Colorado, USA. https://doi.org/10.7265/N5-RGI-60.
Romanovsky, V.V., Tashbaeva, S., Crétaux, J.F., Calmant, S., Drolon, V., 2013. The Closed Lake Issyk-Kul as an Indicator of Global Warming in Tien-Shan.
Rupper, S., Roe, G., Gillespie, A., 2009. Spatial patterns of Holocene glacier advance and retreat in Central Asia. Quat. Res. 72 (3), 337–346.
Sadyrov, S., Tanaka, K., Satylkanov, R., Khujanazarov, T., Touge, Y., Fujita, K., 2024. Modelling runoff components and hydrological processes in glaciated catchments of the inner Tien-Shan, Kyrgyzstan. Front. Earth Sci. 11, 1306476.
Saft, M., Peel, M.C., Western, A.W., Perraud, J.-M., Zhang, L., 2016. Bias in streamflow projections due to climate-induced shifts in catchment response. Geophys. Res. Lett. 43 (4), 1574–1581. https://doi.org/10.1002/2015gl067326.
Sakai, A., 2019. Brief communication: updated GAMDAM glacier inventory over high-mountain Asia. Cryosphere 13, 2043–2049.
Sakai, A., Fujita, K., 2017. Contrasting glacier responses to recent climate change in high-mountain Asia. Sci. Rep. 7 (1), 13717. https://doi.org/10.1038/s41598-017-14256-5.
Saks, T., Pohl, E., Machguth, H., Dehecq, A., Barandun, M., Kenzhebaev, R., et al., 2022. Glacier runoff variation since 1981 in the upper Naryn river catchments, Central Tien Shan. Front. Environ. Sci. 9, 780466.
Schaner, N.A., Voisin, N., Nijssen, B., Lettenmaier, D.P., 2012. The contribution of glacier melt to streamflow. Environ. Res. Lett. 7 (3), 034029. https://doi.org/10.1088/1748-9326/7/3/034029.
Sellers, P., Mintz, Y., Sud, Y. e al, Dalcher, A., 1986. A simple biosphere model (SiB) for use within general circulation models. J. Atmos. Sci. 43, 505–531.
Sellers, P., Randall, D., Collatz, G., Berry, J., Field, C., Dazlich, D., Zhang, C., Collelo, G., Bounoua, L., 1996. A revised land surface parameterisation (SiB2) for atmospheric GCMs. Part I: model formulation. J. Clim. 9, 676–705.
Shannon, S., Payne, A., Freer, J., Coxon, G., Kauzlaric, M., Kriegel, D., Harrison, S., 2023. A snow and glacier hydrological model for large catchments–case study for the Naryn River, central Asia. Hydrol. Earth Syst. Sci. 27 (2), 453–480.
Sidle, R.C., 2021. Strategies for smarter catchment hydrology models: incorporating scaling and better process representation. Geoscience Letters 8 (1), 24.
Siegfried, T., Bernauer, T., Guiennet, R., Sellars, S., Robertson, A.W., Mankin, J., et al., 2012. Will climate change exacerbate water stress in Central Asia? Climatic Change 112, 881–899.
Tanaka, K., 2004. Development of the New Land Surface Scheme SiBUC Commonly Applicable to Basin Water Management and Numerical Weather Prediction Model. Graduate School of Engineering, Kyoto University, p. 289. Doctoral Dissertation.
Teutschbein, C., Seibert, J., 2010. Regional climate models for hydrological impact studies at the catchment scale: a review of recent modeling strategies. Geography Compass 4 (7), 834–860.
Teutschbein, C., Seibert, J., 2012. Bias correction of regional climate model simulations for hydrological climate-change impact studies: review and evaluation of different methods. J. Hydrol. 456, 12–29.
Thirel, G., Andreassian, V., Perrin, C., 2015. On the need to test hydrological models under changing conditions. Hydrol. Sci. J. 60 (7 –8), 1165–1173. https://doi.org/10.1080/02626667.2015.1050027.
Unger-Shayesteh, K., Vorogushyn, S., Farinotti, D., Gafurov, A., Duethmann, D., Mandychev, A., et al., 2013. What do we know about past changes in the water cycle of Central Asian headwaters? A review. Global Planet. Change 110, 4–25. https://doi.org/10.1016/j.gloplacha.2013.02.004.
Van Tricht, L., Huybrechts, P., 2023. Modelling the historical and future evolution of six ice masses in the Tien Shan, Central Asia, using a 3D ice-flow model. Cryosphere 17 (10), 4463–4485.
Van Tricht, L., Paice, C.M., Rybak, O., Satylkanov, R., Popovnin, V., Solomina, O., Huybrechts, P., 2021. Reconstruction of the historical (1750–2020) mass balance of bordu, kara-batkak and sary-tor glaciers in the inner tien Shan, Kyrgyzstan. Front. Earth Sci. 9, 734802.
Verzano, K., Barlund, I., Florke, M., Lehner, B., Kynast, E., Voß, F., Alcamo, J., 2012. Modeling variable river flow velocity on continental scale: current situation and climate change impacts in Europe. J. Hydrol. 424–425, 238–251. https://doi.org/10.1016/j.jhydrol.2012.01.005.
Wegerich, K., Van Rooijen, D., Soliev, I., Mukhamedova, N., 2015. Water security in the Syr darya basin. Water 7 (9), 4657–4684.
Wilby, R.L., Harris, I., 2006. A framework for assessing uncertainties in climate change impacts: low-flow scenarios for the River Thames. UK. Water Resour. Res. 42 (2). https://doi.org/10.1029/2005wr004065.
Yan, X., Zhang, Q., Ren, X., Wang, X., Yan, X., Li, X., et al., 2022. Climatic change characteristics towards the "warming–wetting" trend in the pan-central-asia arid region. Atmosphere 13 (3), 467. https://doi.org/10.3390/atmos13030467.
Zhao, Q., Ye, B., Ding, Y., Zhang, S., Yi, S., Wang, J., Shangguan, D., Zhao, C., Han, H., 2013. Coupling a glacier melt model to the Variable Infiltration Capacity (VIC) model for hydrological modeling in north-western China. Environ. Earth Sci. 68, 87–101. https://doi.org/10.1007/s12665-012-1718-8.
Zou, S., Jilili, A., Duan, W., Maeyer, P.D., de Voorde, T.V., 2019. Human and natural impacts on the water resources in the Syr darya River Basin, central Asia. Sustainability 11 (11), 3084.